Desalination and Water Treatment
www.deswater.com
doi: 10.1080/19443994.2015.1026284

57 (2016) 9190–9202
April

Taylor & Francis
Taylor & Francis Group

Investigation on the effects of heat capacity on the theoretical analysis of single slope passive solar still

V. Sivakumar[a,*], E. Ganapathy Sundaram[b], M. Sakthivel[c]

[a]*Department of Mechanical Engineering, R.M.K. Engineering College, Chennai 601206, India, email: vsk.mech@rmkec.ac.in*
[b]*Department of Mechanical Engineering, Velammal Engineering College, Chennai 600066, India, email: ganapathy_sundar@yahoo.com*
[c]*Department of Mechanical Engineering, INFO Institute of Engineering, Coimbatore 641107, India, email: sakthivelm1962@gmail.com*

Received 26 October 2014; Accepted 3 March 2015

ABSTRACT

Surfaces used for evaporation and condensation play a vital role in the performance of single slope passive solar still. To reach the optimum design, many experimental and numerical studies have been done on different configurations of solar stills by examining the effect of climatic, operational and design parameters of solar still components on its performance. Majority of those investigations have not taken into account the heat capacity of the basin and glass cover for simplification of mathematical model. The heat transfer and thermal losses from the components of a solar still are influenced by the thermal properties like heat capacity, absorptance and thermal conductivity of its components. In this observation, an attempt has been made to develop a mathematical model, which is used to find the effect of heat capacity of the basin and glass cover on the performance and exergy destruction of single slope passive solar still.

Keywords: Passive solar still; Heat capacity; Mathematical model; Exergy destruction

1. Introduction

Potable water is the essence of life and it is the most important constituent of our environment. Obtaining fresh and healthy water is still one of the major problems in different parts of the world, especially in arid and secluded areas. Solar still is a simple device which converts brackish water into potable water using solar energy. The easily available solar energy is clean, plentiful and renewable. Solar stills can be used for low capacity applications and self-reliant water supply system [1]. Solar stills are cheap and have low maintenance cost, but have the problem of low productivity. Many researchers reviewed the methodologies to improve the performance of the active and passive solar stills [2].

Through a theoretical investigation, a descriptive model of a system can be built to estimate how an unpredictable event could affect this system. Madhlopa [3] theoretically investigated the radiative heat transfer inside a single slope solar still with and without considering optical view factors. The result indicates that radiative heat transfer coefficient between water and glass cover is lower when view factor is considered. Rahbar and Esfahani [4] applied the ability of a 2-D computational fluid dynamics (CFD) simulation in

*Corresponding author.

1944-3994/1944-3986 © 2015 Balaban Desalination Publications. All rights reserved.

estimating the hourly yield of single slope solar still and found that accuracy of the CFD analysis in the prediction of Nusselt number is better than its accuracy in productivity estimation. A numerical simulation was developed to optimize the relationship between capillary film solar still coupled in series with another conventional solar still by Zerrouki et al. [5]. The result shows that the daily production is 54–83% higher than that of the conventional one and is most sensitive to area ratio between the receiving surface of basin liner and evaporator plate.

Ben Halima et al. [6] developed a mathematical model (computer simulation programme-MATLAB software) using mass and heat balance to study the performance of solar still coupled to a compression heat pump and proved an increase in efficiency by 75%. Srivastava and Agrawal [7] analysed the performance of basin type solar still, incorporating multiple low thermal inertia porous absorbers (jute cloth) which are made to float with the help of thermocol insulation. The productivity increase for clear day and cloudy day are 68% and 35%, respectively. An experimental and numerical (Finite Element Method) study was done by Xiong et al. [8] on a new multi-effect solar still with enhanced condensation surface which increased productivity by 40%. A theoretical evaluation on the performance of a stepped solar still using water film cooling over the glass cover was done by El-Samadony and Kabeel [9]. They found that daily productivity increased by 8.2%. They also studied the effect of the thickness of film cooling, flow rate, inlet temperature and wind speed. Mohian and Kianifar [10] studied the effect of basin depth, wind velocity, basin insulation thickness and Reynolds number on the performance of a single basin solar still with a pyramid-shaped glass cover in Mashhad, Iran. The study found that the optimum basin depth, wind velocity, insulation thickness Reynolds number were 5 cm, less than 10 m/s, 9 mm and 35,000, respectively, for the maximum daily yield.

Exergy can be regarded as a measure of the usefulness or quality of energy. The exergy method is useful for improving the efficiency of energy resource use, quantifies the locations, types and magnitudes of wastes and losses. Saidur et al. [11] carried out a comprehensive literature review on exergy analysis of various solar energy applications such as solar photovoltaic, solar pond, solar heating devices, solar water desalination, solar air conditioning and refrigeration, solar drying process and solar power generation. Energy, exergy and thermo-economic analysis of solar distillation systems were reviewed by Ranjan and Kaushik [12]. It is observed that the exergy efficiency of a single effect system is less than 5% of its energy efficiency and this value reached up to 8.5% for an integrated solar still. Shiv Kumar and Tiwari [13] developed an analytical expression for instantaneous exergy efficiency of a shallow basin passive solar still and found a decrease of 21.8% and 36.7% of energy and exergy efficiencies, respectively, when the absorptivity of basin liner decreased from 0.9 to 0.6. The exergy efficiency increased rapidly for wind velocity up to 2 m/s and further increase in wind velocity decreased the exergy efficiency.

The theoretical analysis about exergy destruction in the components of a passive solar still—collector plate, brine and glass cover under steady state conditions—was investigated by Torchia-Nunez et al. [14]. The study revealed exergy efficiency of 12.9, 6 and 5% for the collector, brine and solar still, respectively, for the same exergy input and mentioned that the collector plate showed greater irreversibility rate as compared to brine and glass cover. A theoretical and experimental study about the energy and exergy efficiencies of cascade solar still was carried out by Aghaei Zoori et al. [15]. The study found that 84.17% of the total irreversibility (310.01 W) is shared by the absorber plate (260.97 W), with the second highest contribution from glass cover (43.45 W) and the least contribution from saline water (5.62 W).

The exergy destruction of passive solar still components such as basin liner, saline water and glass cover are evaluated as 3,353, 1,633 and 362 W/m^2/d, respectively, for 1 cm water depth by Ranjan et al. [16] for the climatic conditions of Udaipur. The exergy destruction study carried out by Sivakumar and Ganapathy Sundaram [17] for a single slope passive solar still found that the highest exergy destruction takes place in the basin liner as compared to other components for 1, 1.5, 2 and 2.5 cm water depths. Kianifar et al. [18] conducted experiments in Mashhad (36˚36´ N) by using two units of a pyramid-shaped active (equipped with small fan) and passive (no fan) solar still for revealing exergy and economic analysis. In the passive solar still, for 4 cm water depth, the daily exergy efficiency was found to be 3.06% in summer and 2.43% in winter. For the summer, when the water depth increased from 4 to 8 cm, the daily exergy efficiency decreased from 3.06 to 2.81%.

Many researchers [1,13,16,19–25] have taken the heat capacity of the basin material and glass cover as negligible for their mathematical model. The amount of heat energy stored depends mainly on the specific heat of the material. El-Sebaii et al. [26] were presented transient mathematical models for a single slope single basin solar still with and without phase change material (PCM). The results show that the evaporative heat transfer coefficient is increased by

27% on using 3.3 cm of PCM (stearic acid) beneath the basin liner. The daily productivity of 9.005 (kg/m^2 d) with an efficiency of 85.3% has been obtained with PCM compared to 4.998 (kg/m^2 d) without the PCM. The energy balance equations for the various elements of the still without PCM and with three kinds of PCMs which have different melting temperatures were formulated and numerically solved by Ansari et al. [27]. The obtained results show that the excess energy produced during sunshine times is stored in a PCM and utilized during night. Moreover, it is highlighted that the choice of the PCM depends closely on the maximum temperature of the brackish water. Sakthivel et al. [28] experimentally studied the regenerative solar still with jute cloth as an energy storage material. The regenerative solar still with jute cloth gave 20 and 8% higher cumulative yield and efficiency compared to conventional solar still.

The literature survey about the theoretical investigations on the performance of the solar still, the exergy destruction study and effect of heat storage material on the performance of the solar still which was reported by the above-mentioned researchers motivated us to study the effect of heat capacity of basin and glass cover on exergy destruction of single slope passive solar still. In this aspect, a mathematical model was developed to study the effect of heat capacity of basin and glass cover on the performance of single slope passive solar still. The temperature values of basin, water and glass obtained from the mathematical model are used for calculating the cumulative yield and exergy destruction calculation of various components of the solar still.

2. Mathematical models

In a conventional solar still, main system components are basin, saline water and glass cover. The present mathematical model consists of two parts. The first part is for estimating the temperature of basin, saline water and glass cover without considering heat capacity and by considering heat capacity of basin and glass cover. The second part is the calculation of exergy destruction of the components by the result obtained from the first part of the mathematical model.

2.1. Mathematical model of conventional solar still without considering heat capacity

Mathematical model is developed and energy balance equation is written for each component of solar still separately. Thermal circuit of a single slope conventional solar still is shown in Fig. 1. The heat transfer between different components of solar still is mentioned in thermal circuit.

The following assumptions have been made for writing the energy balance equation:

(1) Inclination of the glass cover is not considered.
(2) Heat capacities of the glass cover and the basin liner are negligible.
(3) The system is in a quasi-steady state condition.
(4) There is no vapour leakage.
(5) The heat capacity of the insulation (bottom and sides of the still) is negligible.

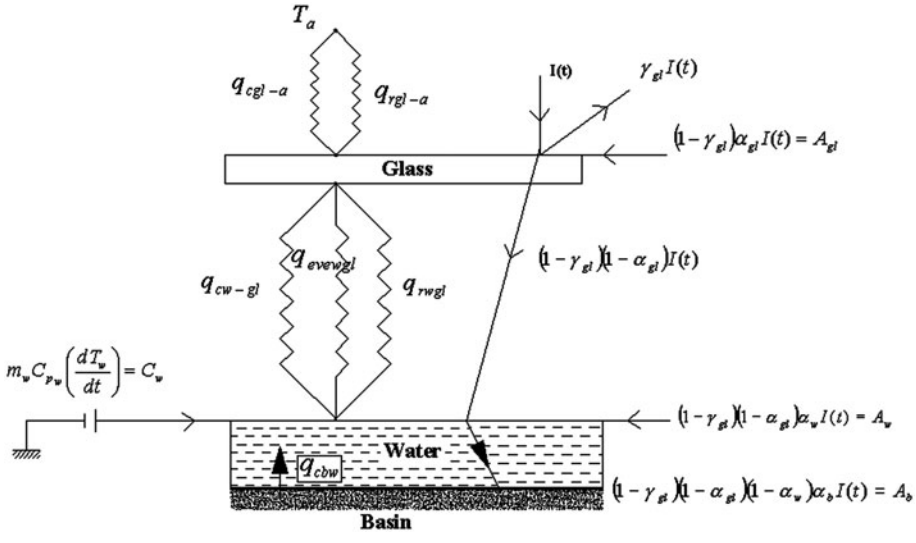

Fig. 1. Thermal circuit diagram for the conventional still with negligible heat capacity of basin and glass cover.

(6) The radiation, convective and evaporative heat losses are linear with the temperature.
(7) The time interval is small and taken as 60 s for the present study
(8) Heat transfer coefficients are temperature dependent.
(9) The physical properties of the water and the glass cover are constant in the operating temperature range.
(10) As absorptivity of water is very low and transmissivity of water is very high, it is assumed that solar radiation directly strikes the basin.
(11) The temperature gradient along the saline water is kept constant.

Energy balance equation for the different components of a conventional still is given below.

2.1.1. Energy balance equation for glass cover without considering heat capacity

Rate of energy absorbed by the glass cover out of solar radiation strikes on it + rate of energy received from water surface by radiation, convection and evaporation = rate of energy lost to atmosphere from glass cover by convection and radiation.

$$I(t)(1-\gamma)\alpha_{gl} + \left(h_{cw-gl} + h_{evaw-gl} + h_{rw-gl}\right)\left(T_w - T_{gl}\right) = \left(h_{cgl-a} + h_{rgl-a}\right)\left(T_{gl} - T_a\right) \quad (1)$$

2.1.2. Energy balance equation for saline water without considering heat capacity

Rate of energy absorbed by the water out of solar radiation strikes on water + rate of heat energy absorbed by water from basin by convection = rate of energy stored in water due to its specific heat + rate of heat transfer from water to glass cover by radiation, convection and evaporation.

$$I(t)(1-\gamma)\left(1-\alpha_{gl}\right)\alpha_w + (h_{cb-w})(T_b - T_w) = M_w C_{p_w}\frac{dT_w}{dt} + \left(h_{cw-gl} + h_{evaw-gl} + h_{rw-gl}\right)\left(T_w - T_{gl}\right) \quad (2)$$

2.1.3. Energy balance equation for basin

Rate of energy absorbed by the basin out of solar radiation strikes on it = rate of heat transfer from basin to water by convection + rate of heat lost from basin to atmosphere through bottom and sides of the still by conduction and convection.

$$I(t)(1-\gamma)\left(1-\alpha_{gl}\right)(1-\alpha_w)\alpha_b = (h_{cb-w})(T_b - T_w) + \left(\frac{K_{ins}}{L_{ins}} + \frac{K_{wood}}{L_{wood}} + h_{c\,wood-a}\right)(T_b - T_a) \quad (3)$$

Eq. (1) can be arranged as

$$T_{gl} = \left(\frac{1}{h_{cw-gl} + h_{evaw-gl} + h_{rw-gl} + h_{cgl-a} + h_{rgl-a}}\right) \times \left[I(t)(1-\gamma)\alpha_{gl} + \left(h_{cw-gl} + h_{evaw-gl} + h_{rw-gl}\right)T_{wi} + \left(h_{cgl-a} + h_{rgl-a}\right)T_a\right] \quad (4)$$

Eq. (2) can be rearranged as

$$\frac{dT_w}{dt} + \frac{\left(h_{cw-gl} + h_{evaw-gl} + h_{rw-gl} + h_{cb-w}\right)}{M_w C_{p_w}}T_w = \frac{1}{M_w C_{p_w}}\left[I(t)(1-\gamma)\left(1-\alpha_{gl}\right)\alpha_w + (h_{cb-w}T_b) + \left(\left(h_{cw-gl} + h_{evaw-gl} + h_{rw-gl}\right)T_{gl}\right)\right] \quad (5)$$

For differential equation in the form of $\frac{dT_w}{dt} + a_1 T_w = C_1$ solution is

$$T_{wi+1} = \frac{C_1}{a_1}(1 - e^{-a_1 t}) + T_{wi}e^{-a_1 t} \quad (6)$$

Eq. (3) can be rearranged as

$$T_{b\,i+1} = \frac{1}{h_{c\,b-w} + \left(\frac{K_{ins}}{L_{ins}} + \frac{K_{wood}}{L_{wood}} + h_{c\,wood-a}\right)} \times \left[\left(I(t)(1-\gamma)\left(1-\alpha_{gl}\right)(1-\alpha_w)\,\alpha_b\right) + h_{c\,b-w}\,T_{wi} + \left(\frac{K_{ins}}{L_{ins}} + \frac{K_{wood}}{L_{wood}} + h_{c\,wood-a}\right)\right] \quad (7)$$

Eqs. (4), (6) and (7) are the set of equations or mathematical model for the conventional still without considering the heat capacity of the basin and glass cover. The steel is considered as material for the basin. The input parameters for these equations include climatic data, operational parameters and thermo-physical properties of the conventional still. The values are shown in Table 1.

By using these thermo-physical parameters, Eqs. (4), (6) and (7) are simplified as follows:

$$T_{gli+1} = 1.041 \times 10^{-3} I(t) + 0.874 T_{wi} + 4.389 \quad (8)$$

Table 1
Thermo-physical properties for conventional still

S. No.	Parameter	Value
1	Area of the basin (A)	1 m^2
2	Mass of the basin (M_b)	8.95 kg
3	Mass of the glass plate (M_g)	4.65 kg
4	Mass of saline water (M_w)	10 kg
5	Specific heat of basin (C_{pb}) [36]	477 J/kg K
6	Specific heat of glass plate (C_{pg}) [36]	840 J/kg K
7	Specific heat of saline water (C_{pw}) [36]	3,930 J/kg K
8	Absorptivity of glass plate (α_g) [15]	0.05
9	Absorptivity of basin (α_b) [15]	0.9
10	Absorptivity of water (α_w) [15]	0.05
11	Transmissivity of glass plate (τ_g) [15]	0.9
12	Transmissivity of water (τ_w) [15]	0.95
13	Effective emissivity (ε_{eff}) [33]	0.82
14	Thickness of wood material (L_{ins})	0.254 m
15	Thickness of insulation material (L_{wood})	0.400 m
16	Thermal conductivity of Insulating material (K_{ins})	0.015 W/m K
17	Thermal conductivity of wood material (K_{wood})	0.15 W/m K
18	Heat transfer coefficient between basin and water surface (h_w) [29]	135 W/m^2 K
19	Overall heat transfer coefficient between basin liner and atmosphere (h_b) [29]	14 W/m^2 K
20	Stefan–Boltzmann constant σ	5.67 x 10^{-8} W/m^2 K^4

$$T_{wi+1} = 1.003 \times 10^{-4} I(t) + 0.745 T_{bi} + 0.084 T_{gi} + 0.162 T_{wi} \quad (9)$$

$$T_{bi+1} = 2.143 \times 10^{-3} I(t) + 0.997 T_{wi} + 0.053 \quad (10)$$

A computer C programme has been developed for solving the above-said linear Eqs. (8) and (9) and non-linear Eq. (10). A time step of 60 s is used in the simulation. Numerical calculations are initiated by assuming the temperatures of different components of the still which are to be equal to their initial temperature at $t = 0$ as T_{wi}, $T_{gl\ i}$ and $T_{bi.}$ Iterations are made for the time step of 60 s for the given input of solar intensity which is assumed to be constant for every 1 h. The temperatures of water, basin and glass cover are calculated for every one hour. After calculating the hourly variation of T_b, T_w and T_{gl}, the hourly yield per unit area is calculated by using the following equation.

$$m = \frac{h_{evaw-gl}(T_w - T_{gl}) \times 3600}{h_{fg}} \left(\frac{kg}{m^2 hr}\right) \quad (11)$$

h_{fg}—Latent heat of evaporation of water. The procedure is repeated with the new values of T_b, T_w and T_{gl} for additional time interval.

2.2. Mathematical model of the conventional still by considering heat capacity

The assumptions made for the development of mathematical model of conventional solar still without considering heat capacity is also considered for the development of mathematical model for this section, except considering the heat capacity of the basin and glass cover (assumption No. 2). Fig. 2 shows the thermal circuit diagram considering the heat capacity of basin and glass cover.

Even though in the previous mathematical model, without considering heat capacity, the heat capacity of the water was considered because the evaporation of water itself considered the heat capacity of water. Hence, variation of water temperature with respect to solar intensity can be taken as Eq. (9).

Then, energy balance for the glass cover and basin by considering its heat capacity are explained below.

2.2.1. Energy balance equation for glass cover by considering heat capacity

Rate of energy absorbed by the glass cover out of solar radiation strikes on it + rate of energy received from water surface by radiation, convection and evaporation = rate of energy stored in glass cover due to its heat capacity + rate of energy lost to the atmosphere from glass cover by convection and radiation.

$$I(t)(1-\gamma)\alpha_{gl} + \left(h_{cw-gl} + h_{evaw-gl} + h_{rw-gl}\right)\left(T_w - T_{gl}\right) = M_{gl}C_{p_{gl}}\frac{dT_{gl}}{dt} + \left(h_{cgl-a} + h_{rgl-a}\right)\left(T_{gl} - T_a\right) \quad (12)$$

$$\frac{dT_{gl}}{dt} + \frac{\left(h_{cw-gl} + h_{evaw-gl} + h_{rw-gl} + h_{cgl-a} + h_{rgl-a}\right)}{M_{gl}C_{p_{gl}}}T_{gl} = \frac{1}{M_{gl}C_{p_{gl}}}\left[I(t) + \left(\left(h_{cw-gl} + h_{evaw-gl} + h_{rw-gl}\right) \times T_w\right) + \left(\left(h_{cgl-a} + h_{rgl-a}\right) \times T_a\right)\right] \quad (13)$$

Hence, solution for Eq. (13) is

$$T_{gli+1} = 5.25 \times 10^{-4} I(t) + 0.43T_{wi} + 0.496T_{gli} + 2.289 \quad (14)$$

2.2.2. Energy balance equation for basin by considering heat capacity

Rate of energy absorbed by the basin out of the solar radiation that strikes on it = rate of energy stored in the basin due to its heat capacity + rate of heat from basin to water by convection + rate of heat lost from basin to atmosphere through the bottom and sides of the still by conduction and convection.

$$I(t)(1-\gamma)\left(1-\alpha_{gl}\right)\left(1-\alpha_w\right)\alpha_b = M_bC_{p_b}\frac{dT_b}{dt} + \left(h_{cb-w}\right)\left(T_b - T_w\right) + \left(\frac{K_{ins}}{L_{ins}} + \frac{K_{wood}}{L_{wood}} + h_{c\,wood-a}\right)\left(T_b - T_a\right) \quad (15)$$

$$\frac{dT_b}{dt} + \frac{\left(\frac{K_{ins}}{L_{ins}} + \frac{K_{wood}}{L_{wood}} + h_{c\,wood-a} + h_{cb-w}\right)}{M_bC_{p_b}}T_b = \frac{1}{M_bC_{p_b}}\left[I(t) + \left(h_{cb-w} \times T_w\right) + \left(\left(\frac{K_{ins}}{L_{ins}} + \frac{K_{wood}}{L_{wood}} + h_{c\,wood-a}\right) \times T_a\right)\right] \quad (16)$$

For the differential Eq. (16), solution is

$$T_{bi+1} = 7.43 \times 10^{-4} I(t) + 0.997T_{wi} + 4.7 \times 10^{-8} T_{bi} + 0.021 \quad (17)$$

Similar to without considering heat capacity, C programme is developed for solving the above-said nonlinear Eqs. (9), (14) and (17). With respect to hourly varying solar intensity, hourly variation of system components temperatures T_b, T_w and T_{gl} are calculated. From these temperatures, hourly yield per unit area is obtained by using Eq. (11). Theoretical hourly yield for different time duration from morning 9.00 am to evening 19:00 h is calculated both with and without considering the heat capacity of the glass cover and basin of the conventional still. Hence, the effects of heat

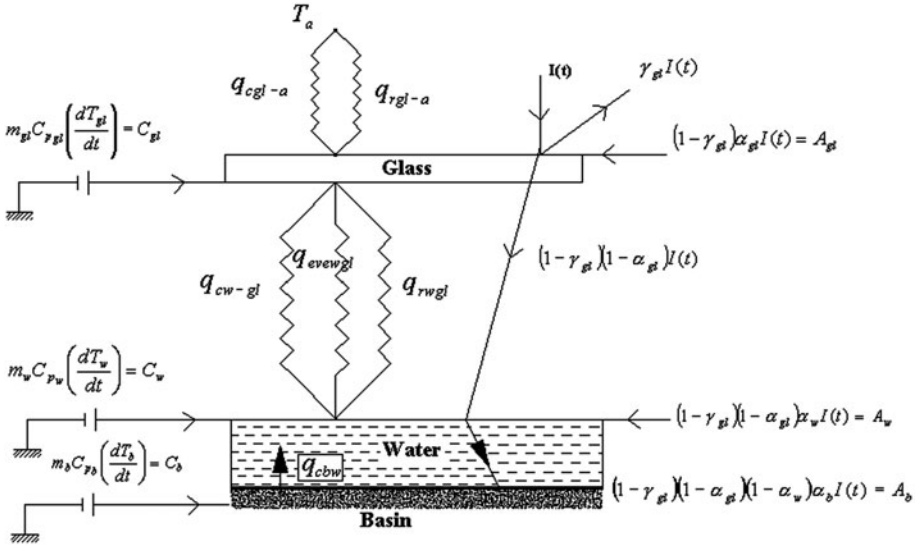

Fig. 2. Thermal circuit diagram with heat capacity of basin and glass cover.

capacity of the basin and glass cover on the performance of the still and exergy destruction are studied.

3. Exergy destruction of solar still components

The combinations of conservation of law of energy and exergy destruction are used for finding exergy balance for any system or its components. The exergy balance Eqs. (18), (22) and (31) of the three main components of the solar still such as basin, saline water and glass cover are given below [17].

3.1. Exergy destruction of basin

The exergy input for the basin is the fraction of solar exergy ($E_{x_{sun}}$) reaching on it. The useful exergy is utilized to raise the temperature of saline water (E_{x_w}) and a little is lost through insulation ($E_{x_{ins.}}$) and the remaining is destroyed ($E_{x_{des.,b}}$).

$$E_{x_{des.,b}} = (\tau_g \tau_w \alpha_b) E_{x_{sun}} - (E_{x_w} + E_{x_{ins.}}) \quad (18)$$

$\tau_g, \tau_w,$ and α_b transmittance of the glass cover, saline water and absorptivity of the basin, respectively [15].

Exergy of the solar radiation on the solar still per unit area, $E_{x_{sun}}$ (W/m^2), is given as:

$$E_{x_{sun}} = I_{t(s)} \left[1 + \frac{1}{3} \left(\frac{T_a}{T_s} \right)^4 - \frac{4}{3} \left(\frac{T_a}{T_s} \right) \right] \quad (19)$$

T_a is the temperature of the atmosphere outside the solar still (K) and T_s is the temperature of the sun (5,777 K).

$$E_{x_w} = h_{cb-w} (T_b - T_w) \left(1 - \frac{T_a}{T_b} \right) \quad (20)$$

where h_{cb-w} [29] is the convective heat transfer coefficient between basin and saline water (W/m^2 K). T_b is the temperature of the basin (K) and T_w is the temperature of the saline water (K).

$$E_{x_{ins.}} = h_b (T_b - T_a) \left(1 - \frac{T_a}{T_b} \right) \quad (21)$$

where h_b [29] is the overall heat transfer coefficient between basin liner and atmosphere (W/m^2 K).

3.2. Exergy destruction of saline water

The exergy input for the saline water is the sum of the fraction of solar exergy ($\tau_g \alpha_w E_{x_{sun}}$) absorbed by water and the useful exergy from the basin which is utilized to raise the temperature of saline water (E_{x_w}). A part of it is utilized as the exergy associated with the heat transfer between saline water surface and the inner side of the glass cover ($E_{x_{t,w-gl}}$) and remaining is destroyed ($E_{x_{des.,w}}$).

$$E_{x_{des.,w}} = (\tau_g \alpha_w) E_{x_{sun}} + E_{x_w} - E_{x_{t,w-gl}} \quad (22)$$

where α_w is the absorptivity of saline water and $E_{x_{t,w-gl}}$ is calculated as follows.

$$E_{x_{t,w-gl}} = E_{x_{eva,w-gl}} + E_{x_{c,w-gl}} + E_{x_{rw-gl}} \quad (23)$$

$E_{x_{eva,w-gl}}, E_{x_{c,w-gl}}$ and $E_{x_{r,w-gl}}$ are the exergy associated with the heat transfer through evaporation, convection and radiation between the saline water surface and the inner side of the glass cover.

$$E_{x_{eva,w-gl}} = h_{eva,\,w-gl} (T_w - T_{gi}) \left(1 - \frac{T_a}{T_w} \right) \quad (24)$$

where $h_{e,w-g}$ is the evaporative heat transfer coefficient between saline water and inner side of the glass cover (W/m^2 K) [30], and T_{gi} is the glass inner surface temperature (K).

$$h_{eva,\,w-gl} = 0.016273\, h_{c,\,w-g} \frac{P_w - P_{gi}}{T_w - T_{gi}} \quad (25)$$

where P_w and P_{gi} are the partial pressures in (N/m^2) for water vapour at water and the inner glass surface temperatures within the still which are given by [31] as:

$$P(T) = \exp \left[25.317 - \frac{5144}{T} \right] \quad (26)$$

$$E_{x_{c,w-gl}} = h_{c,w-gl} (T_w - T_{gi}) \left(1 - \frac{T_a}{T_w} \right) \quad (27)$$

where $h_{c,w-gl}$ is the convective heat transfer coefficient between saline water and inner side of the glass cover (W/m^2 K) [30].

$$h_{c,w-gl} = 0.884\left[T_w - T_{gi} + \frac{(P_w - P_{gi})\,T_w}{268,900 - P_w}\right]^{1/3} \quad (28)$$

$$E_{x_{r,w-gl}} = h_{r,w-gl}(T_w - T_{gi})\left[1 + \frac{1}{3}\left(\frac{T_a}{T_w}\right)^4 - \frac{4}{3}\left(\frac{T_a}{T_w}\right)\right] \quad (29)$$

where $h_{r,w-gl}$ is the radiative heat transfer coefficient between saline water and inner side of the glass cover (W/m^2 K) [32].

$$h_{r,w-gl} = \varepsilon_{eff}\sigma\left(T_w^2 + T_{gi}^2\right)(T_w + T_{gi}) \quad (30)$$

ε_{eff} is the effective emissivity [33] and σ is the Stefan–Boltzmann constant taken as 5.67 x 10^{-8} W/m^2 K^4.

3.3. Exergy destruction of glass cover

The exergy input for the glass cover is the sum of the fraction of solar exergy ($\alpha_b E_{x_{sun}}$) absorbed by glass cover and the exergy associated with the heat transfer between saline water surface and the inner side of the glass cover ($E_{x_{t,w-gl}}$). A part of this exergy is lost to the atmosphere by convection and radiation heat transfer and remaining is destroyed ($E_{x_{des.,gl}}$).

$$E_{x_{des.,gl}} = \alpha_g E_{x_{sun}} + E_{x_{t,w-gl}} - E_{x_{t,gl-a}} \quad (31)$$

where α_g is the absorptivity of glass cover and $E_{x_{t,gl-a}}$ is calculated as follows.

$$E_{x_{t,gl-a}} = E_{x_{c,gl-a}} + E_{x_{r,gl-a}} \quad (32)$$

$$E_{x_{c,gl-a}} = h_{c,gl-a}(T_{go} - T_a)\left(1 - \frac{T_a}{T_{go}}\right) \quad (33)$$

$$h_{c,gl-a} = 5.7 + 3.8V \quad (34)$$

V = wind speed in m/s.

where $h_{c,gl-a}$ is the convective heat transfer coefficient between glass cover and atmosphere (W/m^2 K) [34] and T_{go} is the outer glass temperature (K).

$$E_{x_{r,gl-a}} = h_{r,gl-a}(T_{go} - T_a)\left[1 + \frac{1}{3}\left(\frac{T_a}{T_{go}}\right)^4 - \frac{4}{3}\left(\frac{T_a}{T_{go}}\right)\right] \quad (35)$$

where $h_{r,gl-a}$ is the radiative heat transfer coefficient between glass cover and atmosphere (W/m^2 K) [34].

$$h_{r,gl-a} = \frac{\varepsilon_{eff}\sigma\left(T_{go}^4 - T_{sky}^4\right)}{T_{go} - T_{sky}} \quad (36)$$

$$T_{sky} = 0.0552\ T_a^{1/5} \quad (37)$$

T_{sky} is the sky temperature (K) [35].

4. Results and discussion

The mathematical equations are derived to study the effect of heat capacity of the basin and glass cover on its temperature. The C programme is used to solve the mathematical equations and find out the temperature of the solar still components. The effects of variation of solar still components temperature on the yield and exergy destruction are also studied.

Fig. 3 shows the variation of basin temperatures with and without heat capacity. The temperature of the basin liner considering the heat capacity is lower compared to considering heat capacity up to 13:00 h, due to the heat storing capacity of the basin. Henceforth, from 13:00 h, the temperature of the basin is higher in the case of considering heat capacity due to liberation of heat stored in the basin during 9:00–13.00 h. The maximum temperature attained by the basin with and without heat capacity is 82 and 85°C, respectively.

Heat capacity of the saline water plays a vital role in the mathematical model. Variation of the saline water temperature with and without considering heat capacity of basin and glass cover is shown in Fig. 4. It is noticed that after 14:00 h, temperature of the saline

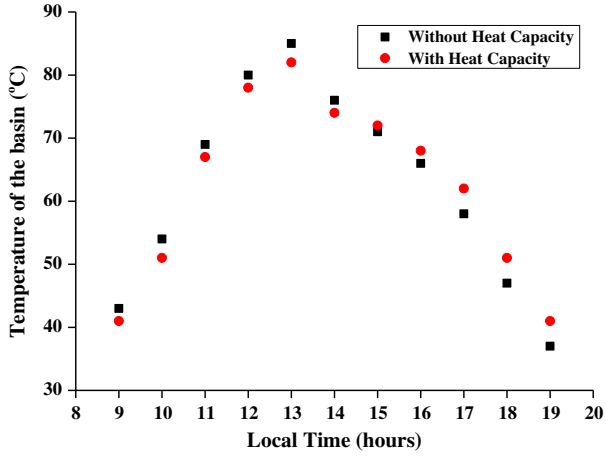

Fig. 3. Hourly variation of temperature of the basin with and without considering heat capacity.

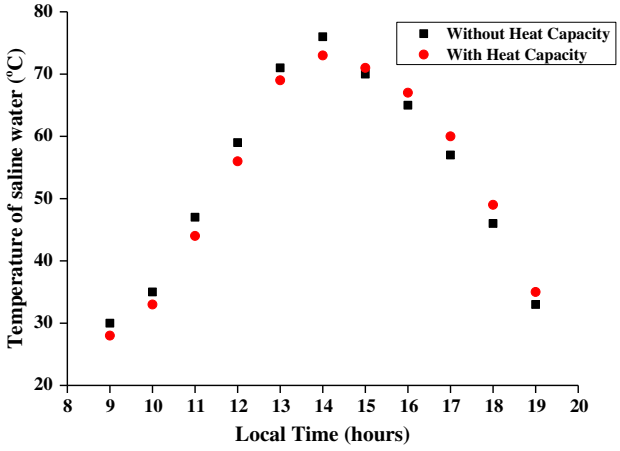

Fig. 4. Hourly variation of temperature of saline water with and without considering heat capacity.

water with heat capacity is higher than that of the temperature of saline water without considering heat capacity. This is owing to the heat from the solar radiation incident on the water and additional heat transferred from basin to water. This increases saline water temperature, and thus results in more yield. The maximum temperature of the saline water obtained with heat capacity is 73˚C.

The temperature of the condensation surface has a great importance on the still's performance. Temperature of the glass cover must be lower than that of the water vapour for condensation. Hourly variation of glass temperature with and without considering heat capacity is presented in Fig. 5. It is inferred from Fig. 5 that after 14.00 h, the temperature of the glass cover is higher when considering heat capacity. This

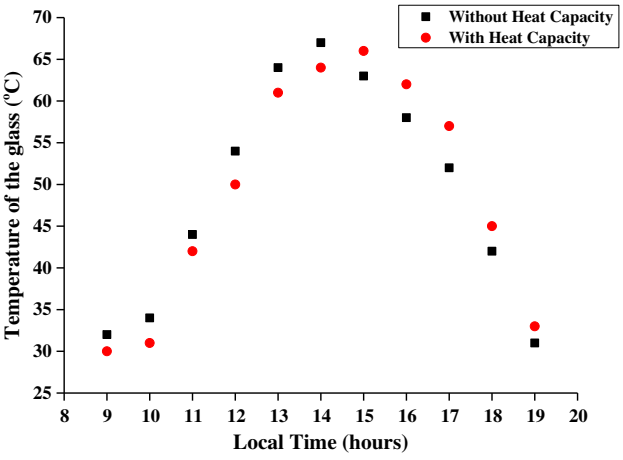

Fig. 5. Hourly variation of temperature of the glass with and without considering heat capacity.

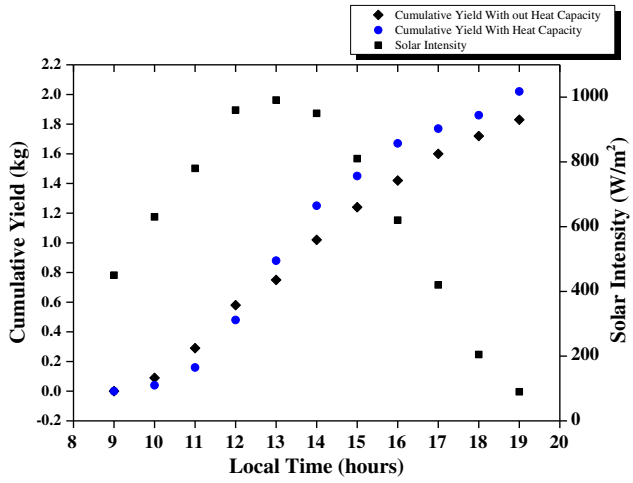

Fig. 6. Hourly variation of solar intensity, cumulative yield with and without considering heat capacity.

is due to liberation of heat stored inside the glass cover and higher evaporative heat transfer from the saline water. The temperature difference between the saline water and glass plays a vital role in productivity of the solar still. The variation of solar intensity and cumulative yield with different time is shown in Fig. 6. The values of solar intensity cited in this model are referred from previous experimental analysis [17]. The analysis found that the cumulative yield with considering heat capacity (2.02 kg/d) is higher than the yield obtained without considering heat capacity (1.8 kg/d). The higher cumulative yield with considering heat capacity could be due to considering heat storage capacity of basin which will increase the yield. The solar still with heat storage system gives higher yield than the conventional solar still [26–28].

Exergy analysis is a powerful indicative tool for thermal system performance evaluation. Exergy flow diagram of the single slope passive solar still is shown in Fig. 7. The present analysis inferred that the exergy destruction in the basin is maximum compared to exergy destruction of saline water and glass cover. The effect of heat capacity on exergy destruction of the basin is shown in Fig. 8. Referring to Fig. 8, it is clear that the values of exergy destruction for without considering heat capacity is lower till 12 noon from the time of observation; after that, the values are higher than with considering heat capacity. This could be due to higher basin liner temperature after 13.00 h which leads to more amount of useful work. In the earlier hours, heat energy is predominantly stored in the basin rather than utilized as useful energy (for evaporation); this could be due to considering heat storage of the basin. On the other hand, lower

temperature difference between the basin and the water results in less useful energy, thus increasing the exergy destruction in the basin. The fluctuations in Fig. 8 are due to exergy inertia. The maximum exergy destruction of the basin with and without heat capacity is 525.45 and 598 W/m^2, respectively, at 14.00 h.

The exergy destruction value of saline water is intermediate to basin and glass cover. The trend of exergy destruction of saline water with respect to time is shown in Fig. 9. Heat capacity of the water is considered in both the cases. It is observed that by considering heat capacity of basin and glass cover, the exergy destruction of saline water is low up to 11.00 h, due to lower water temperature and after that the value is higher, and this could be due to higher water temperature. The maximum exergy destruction of saline water by considering heat capacity is 318.82 W/m^2. Decrease in heat flux rates and narrowing temperature between basin and temperature is responsible for increase in exergy destruction of saline water; moreover, the exergy of water is the major source of distillation [14].

The least exergy destruction is identified in the glass cover. Fig. 10 illustrates the exergy destruction of glass with and without considering heat capacity. The maximum exergy destruction of glass with and without heat capacity is 39.51 and 44.91 W/m^2, respectively, at 12.00 noon.

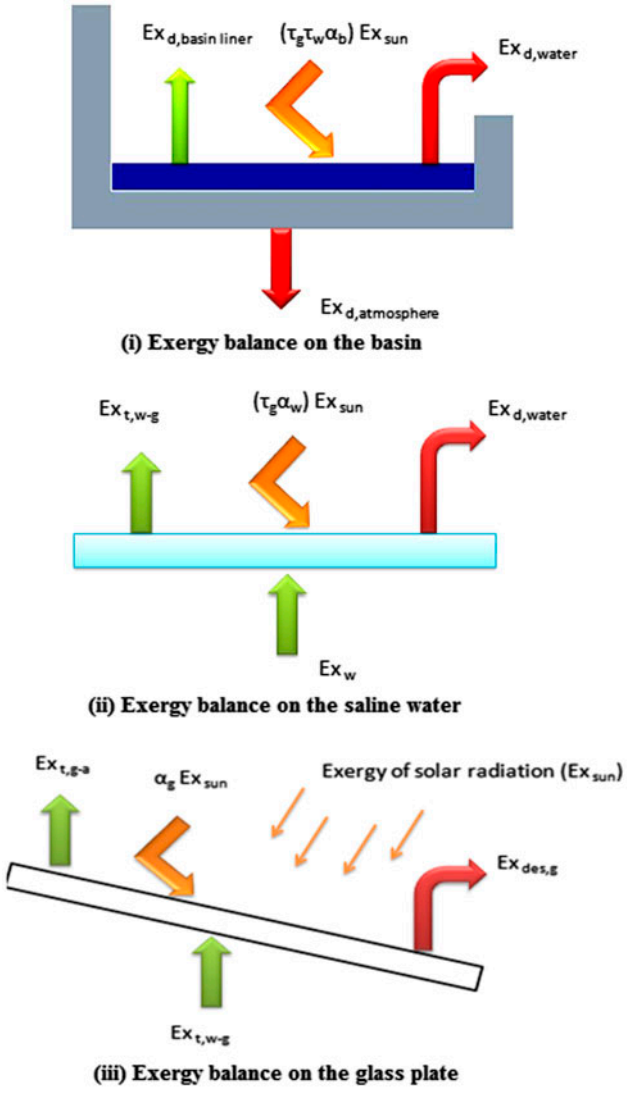

Fig. 7. Schematic diagrams showing the exergy transfers in the components of a single slope passive solar still. (i) Exergy balance on the basin. (ii) Exergy balance on the saline water. (iii) Exergy balance on the glass cover.

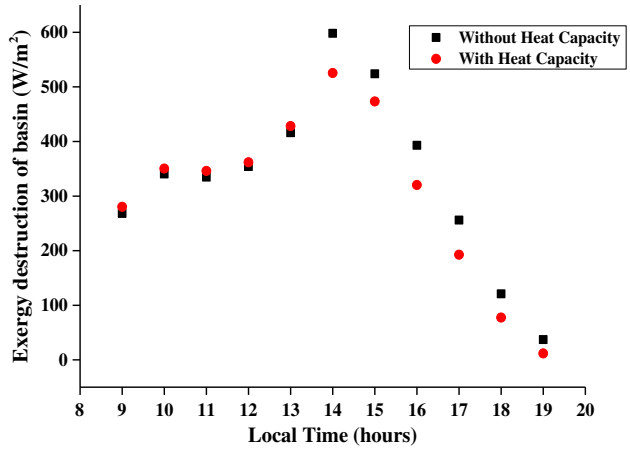

Fig. 8. Hourly variation of exergy destruction of basin with and without considering heat capacity.

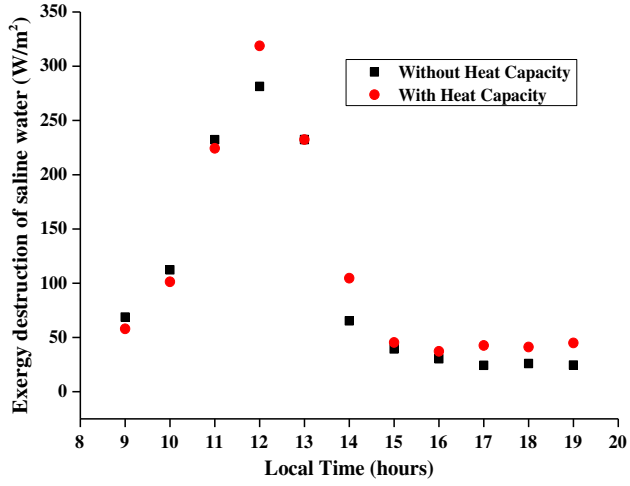

Fig. 9. Hourly variation of exergy destruction of saline water with and without considering heat capacity.

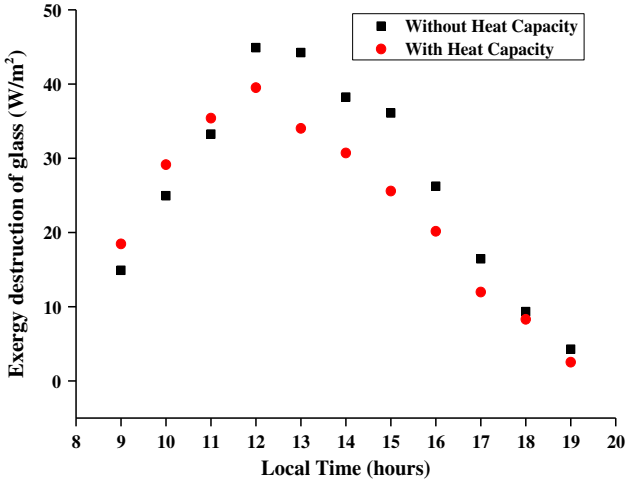

Fig. 10. Hourly variation of exergy destruction of glass with and without considering heat capacity.

The total exergy destruction of various solar still components is represented in Fig. 11. The total exergy destruction by considering heat capacity of basin, saline water and glass cover are 3,367.67, 1,250.8 and 244.21 W/m^2, respectively. The total exergy destruction of basin, saline water and glass are 3,642.23, 1,137.1 and 290.2 W/m^2, respectively, without considering the heat capacity of basin and glass cover. Similar trends of exergy destruction for without considering the heat capacity of basin and glass cover are obtained in the experiments. The values obtained from the experiment are 3,343.86 and 232.87 W/m^2/d for basin and glass cover, respectively [17]. The total exergy destruction decreased by 274.56 and 45.99 W/m^2 for basin and glass cover, respectively, by considering heat capacity. On contrary, for saline water the value is increased by 113.7 W/m^2. This is owing to the fact that negative effect of exergy transfer on one process sometimes produces useful effect on other processes if taken in totality [16].

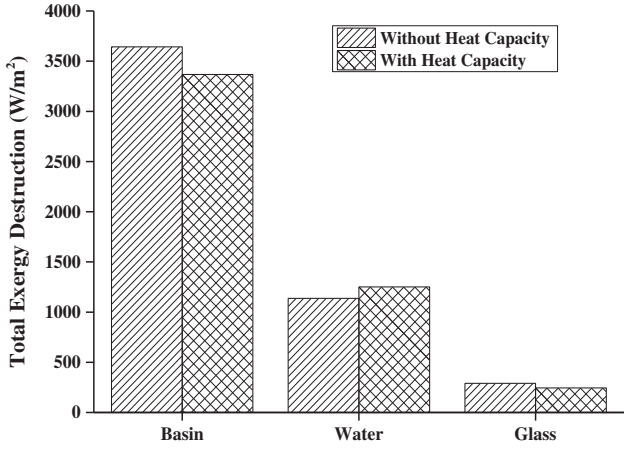

Fig. 11. Comparison of total exergy destruction of solar still components with and without considering heat capacity.

5. Conclusions

The present theoretical investigation indicates the importance of heat capacity consideration of basin and glass cover on the performance of solar still and exergy destruction calculation for solar still components. The following conclusions can be drawn:

(1) The temperature of solar still components considering heat capacity is low up to noon and after that the temperature is higher by considering heat capacity of basin and glass plate.
(2) The cumulative yield of solar still increases by 10.38% with considering heat capacity.
(3) The maximum total exergy destruction (3,642.23 W/m^2) is found in the basin and the minimal is from glass (290.2 W/m^2) without considering heat capacity.
(4) The total exergy destruction by considering heat capacity of basin and glass decreases by 7.53 and 15.84%, respectively; on contrary, an increase of 9.99% occurred for saline water.
(5) Instead of using various heat storage materials to improve the performance of solar still, the heat capacity of the various components of the still will be considered after further studies.

Nomenclature

M_w — mass of saline water (kg)
M_b — mass of basin (kg)
m — hourly distillate yield (kg)
C_{p_w} — specific heat of water (J/kg K)
C_{p_b} — specific heat of basin (J/kg K)
C_{p_g} — specific heat of glass (J/kg K)
K_{ins} — thermal conductivity of insulation material (W/m°C)
K_{wood} — thermal conductivity of wood (W/m°C)
L_{ins} — thickness of insulation (m)
L_{wood} — thickness of wood material (m)
h_{fg} — latent heat of vaporization (J/kg)
A — basin area of solar still (m^2)
$I(t)$ — hourly incident solar radiation (W/m^2)
T_a — ambient air temperature (K)
T_w — water temperature (K)
T_b — basin temperature (K)

T_{gi} — inner glass temperature (K)
T_{go} — outer glass temperature (K)
T_{sky} — sky temperature (K)
$E_{x_{des.,b}}$ — exergy destruction from basin liner (W/m^2)
$E_{x_{des.,w}}$ — exergy destruction from saline water (W/m^2)
$E_{x_{des.,gl}}$ — exergy destruction from glass cover (W/m^2)
$E_{x_{ins.}}$ — exergy loss through insulation (W/m^2)
E_{x_w} — exergy utilized to heat saline water (W/m^2)
$E_{x_{t,w-gl}}$ — total exergy associated with saline water and glass cover (W/m^2)
$E_{x_{e,w-gl}}$ — exergy associated with saline water and glass cover through evaporation (W/m^2)
$E_{x_{c,w-gl}}$ — exergy associated with saline water and glass cover through convection (W/m^2)
$E_{x_{r,w-gl}}$ — exergy associated with saline water and glass cover through radiation (W/m^2)
$E_{x_{t,gl-a}}$ — total exergy associated with glass cover and atmosphere (W/m^2)
$E_{x_{c,gl-a}}$ — exergy associated with glass cover and atmosphere through convection (W/m^2)
$E_{x_{r,gl-a}}$ — exergy associated with glass cover and atmosphere through radiation (W/m^2)
$h_{cwood-a}$ — convective heat transfer between wood and atmosphere (W/m^2 K)
$h_{c,b-w}$ — convective heat transfer between basin and water (W/m^2 K)
h_b — overall heat transfer between basin and atmosphere (W/m^2 K)
$h_{eva,w-gl}$ — evaporative heat transfer coefficient between saline water and glass cover (W/m^2 K)
$h_{c,w-gl}$ — convective heat transfer coefficient between saline water and glass cover (W/m^2 K)
$h_{r,w-gl}$ — radiative heat transfer coefficient between saline water and glass cover (W/m^2 K)
$h_{c,gl-a}$ — convective heat transfer coefficient between glass cover and atmosphere (W/m^2 K)
$h_{r,gl-a}$ — radiative heat transfer coefficient between glass cover and atmosphere (W/m^2 K)
V — wind velocity in (m/s)

Symbols

α_g — absorptivity of glass cover
α_b — absorptivity of basin liner
α_w — absorptivity of water
τ_g — transmissivity of glass cover
τ_w — transmissivity of water
γ — reflectivity of glass cover
ε_{eff} — effective emissivity
σ — Stefan–Boltzmann constant
A_b — absorptance of basin
A_w — absorptance of saline water
A_{gl} — absorptance of glass cover

References

[1] A. Kaushal, Varun, Solar stills: A review, Renewable Sustainable Energy Rev. 14 (2010) 446–453.
[2] V. Sivakumar, E. Ganapathy Sundaram, Improvement techniques of solar still efficiency: A review, Renewable Sustainable Energy Rev. 28 (2013) 246–264.
[3] A. Madhlopa, Modelling radiative heat transfer inside a basin type solar still, Appl. Therm. Eng. 73 (2014) 705–709.
[4] N. Rahbar, J.A. Esfahani, Productivity estimation of a single-slope solar still: Theoretical and numerical analysis, Energy 49 (2013) 289–297.
[5] M. Zerrouki, N. Settou, Y. Marif, M.M. Belhadj, Simulation study of a capillary film solar still coupled with a conventional solar still in south Algeria, Energy Convers. Manage. 85 (2014) 112–119.
[6] H. Ben Halima, N. Frikha, R. Ben Slama, Numerical investigation of a simple solar still coupled to a compression heat pump, Desalination 337 (2014) 60–66.
[7] P.K. Srivastava, S.K. Agrawal, Experimental and theoretical analysis of single sloped basin type solar still consisting of multiple low thermal inertia floating porous absorbers, Desalination 311 (2013) 198–205.
[8] J. Xiong, G. Xie, H. Zheng, Experimental and numerical study on a new multi-effect solar still with enhanced condensation surface, Energy Convers. Manage. 73 (2013) 176–185.
[9] Y.A.F. El-Samadony, A.E. Kabeel, Theoretical estimation of the optimum glass cover water film cooling parameters combinations of a stepped solar still, Energy 68 (2014) 744–750.
[10] O. Mahian, A. Kianifar, Mathematical modelling and experimental study of a solar distillation system, Proc. Inst. Mech. Eng. J. Mech. Eng. Sci. 225 (2011) 1203–1212.
[11] R. Saidur, G. BoroumandJazi, S. Mekhlif, M. Jameel, Exergy analysis of solar energy applications, Renewable Sustainable Energy Rev. 16 (2012) 350–356.
[12] K.R. Ranjan, S.C. Kaushik, Energy, exergy and thermo-economic analysis of solar distillation systems: A review, Renewable Sustainable Energy Rev. 27 (2013) 709–723.
[13] S. Kumar, G.N. Tiwari, Analytical expression for instantaneous exergy efficiency of a shallow basin passive solar still, Int. J. Therm. Sci. 50 (2011) 2543–2549.
[14] J.C. Torchia-Nunez, M.A. Porta-Gandara, J.G. Cervantes-de Gortari, Exergy analysis of a passive solar still, Renewable Energy 33 (2008) 608–616.
[15] H. Aghaei Zoori, F. Farshchi Tabrizi, F. Sarhaddi, F. Heshmatnezhad, Comparison between energy and exergy efficiencies in a weir type cascade solar still, Desalination 325 (2013) 113–121.
[16] K.R. Ranjan, S.C. Kaushik, N.L. Panwar, Energy and exergy analysis of passive solar distillation systems, Int. J. Low Carbon Technol. (2013) 1–11. Available from: <http://ijlct.oxfordjournals.org/content/early/2013/09/26/ijlct.ctt069.full.pdf±html>.
[17] V. Sivakumar, E. Ganapathy Sundaram, Energy and exergy analysis of single slope passive solar still: An experimental investigation, Desalin. Water Treat. (2014), doi: 10.1080/19443994.2014.928794.
[18] A. Kianifar, S. Zeinali Heris, O. Mahian, Exergy and economic analysis of a pyramid-shaped solar water purification system: Active and passive cases, Energy 38 (2012) 31–36.
[19] B. Janarthanan, J. Chandrasekaran, S. Kumar, Performance of floating cum tilted-wick type solar still with

the effect of water flowing over the glass cover, Desalination 190 (2006) 51–62.
[20] A.A. El-Sebaii, M.R.I. Ramadan, S. Aboul-Enein, N. Salem, Thermal performance of a single-basin solar still integrated with a shallow solar pond, Energy Convers. Manage. 49 (2008) 2839–2848.
[21] G.N. Tiwari, V. Dimri, A. Chel, Parametric study of an active and passive solar distillation system: Energy and exergy analysis, Desalination 242 (2009) 1–18.
[22] A.A. El-Sebaii, S.J. Yaghmour, F.S. Al-Hazmi, A.S. Faidah, F.M. Al-Marzouki, A.A. Al-Ghamdi, Active single basin solar still with a sensible storage medium, Desalination 249 (2009) 699–706.
[23] K. Sampathkumar, T.V. Arjunan, P. Pitchandi, P. Senthilkumar, Active solar distillation—A detailed review, Renewable Sustainable Energy Rev. 14 (2010) 1503–1526.
[24] V.K. Dwivedi, G.N. Tiwari, Thermal modeling and carbon credit earned of a double slope passive solar still, Desalin. Water Treat. 13 (2010) 400–410.
[25] V.K. Dwivedi, G.N. Tiwari, Experimental validation of thermal model of a double slope active solar still under natural circulation mode, Desalination 250 (2010) 49–55.
[26] A.A. El-Sebaii, A.A. Al-Ghamdi, F.S. Al-Hazmi, A.S. Faidah, Thermal performance of a single basin solar still with PCM as a storage medium, Appl. Energy 86 (2009) 1187–1195.
[27] O. Ansari, M. Asbik, A. Bah, A. Arbaoui, A. Khmou, Desalination of the brackish water using a passive solar still with a heat energy storage system, Desalination 324 (2013) 10–20.
[28] M. Sakthivel, S. Shanmugasundaram, T. Alwarsamy, An experimental study on a regenerative solar still with energy storage medium—Jute cloth, Desalination 264 (2010) 24–31.
[29] Y.H. Zurigat, M.K. Abu-Arabi, Modeling and performance analysis of a regenerative solar desalination unit, Appl. Therm. Eng. 24 (2004) 1061–1072.
[30] R.V. Dunkle, Solar water distillation, the roof type solar still and a multi effect diffusion still, in: Proceedings of International Heat Transfer, Part 5, Internal Developments in Heat Transfer, ASME, University of Colorado, Boulder, CO, 1961, pp. 895–902.
[31] J.L. Fernández, N. Chargoy, Multi stage indirectly heated solar still, Sol. Energy 44(4) (1990) 215–223.
[32] S.K. Shukla, V.P.S. Sorayan, Thermal modeling of solar stills: An experimental validation, Renewable Energy 30 (2005) 683–699.
[33] E. Sartori, Solar still versus solar evaporator: A comparative study between their thermal behaviors, Sol. Energy 56(2) (1996) 199–206.
[34] W.H. McAdams, Heat Transmission, third ed., McGraw-Hill, New York, NY, 1954.
[35] W.C. Swinbank, Long-wave radiation from clear skies, Q. J. Royal Meteorol. Soc. 89 (1963) 339–348.
[36] S.M. Radwan, A.A. Hassanain, M.A. Abu-Zeid, Single slope solar still for sea water distillation, World Appl. Sci. J. 7 (4) (2009) 485–497.